British Journal of Pharmacology (2003) 140, 202–210 
www.nature.com/bjp

# 2′, 3′-*O*-(2,4,6,Trinitrophenyl)-ATP and A-317491 are competitive antagonists at a slowly desensitizing chimeric human $P2X_3$ receptor

[1]Torben R. Neelands, [1,2]Edward C. Burgard, [1]Marie E. Uchic, [1]Heath A. McDonald, [1]Wende Niforatos, [1]Connie R. Faltynek, [1]Kevin J. Lynch, & *,[1]Michael F. Jarvis

[1]Neuroscience Research, Global Pharmaceutical Research and Development, Abbott Laboratories, R04PM, AP9A, Abbott Park, IL 60064-6123, U.S.A.

**1** Rapid desensitization of ligand-gated ion channel receptors can alter the apparent activity of receptor modulators, as well as make detection of fast-channel activation difficult. Investigation of the antagonist pharmacology of ATP-sensitive homomeric $P2X_3$ receptors is limited by agonist-evoked fast-desensitization kinetics.

**2** In the present studies, chimeric receptors were created using the coding sequence for the N-terminus and the first transmembrane domain of either the nondesensitizing human $P2X_{2a}$ or fast-desensitizing $P2X_3$ receptor joined to the sequence encoding the extracellular loop, second transmembrane domain, and C-terminus of the other receptor (designated $P2X_{2-3}$ and $P2X_{3-2}$, respectively). These clones were stably transfected into 1321N1 astrocytoma cells for biophysical and pharmacological experiments using both electrophysiological and calcium-imaging methods.

**3** Chimeric $P2X_{2-3}$ and $P2X_{3-2}$ receptors were inwardly rectifying and agonist responses showed desensitization properties similar to the wild-type human $P2X_{2a}$ and $P2X_3$ receptors, respectively.

**4** The $P2X_{2-3}$ chimera displayed an agonist pharmacological profile similar to the $P2X_3$ wild-type receptor being activated by low concentrations of both ATP and α,β-meATP. In contrast, the $P2X_{3-2}$ chimera had markedly reduced sensitivity to both agonists.

**5** The $P2X_3$ receptor antagonists TNP-ATP and A-317491 were shown to be potent, competitive antagonists of the $P2X_{2-3}$ chimera ($K_i = 2.2$ and 52.1 nM, respectively), supporting the hypothesis that rapid receptor desensitization can mask the competitive antagonism of wild-type homomeric $P2X_3$ receptors.

*British Journal of Pharmacology* (2003) **140,** 202–210. doi:10.1038/sj.bjp.0705411

**Keywords:** Purinergic receptors; $P2X_2$; $P2X_3$; chimeras; desensitization; competitive antagonist; TNP-ATP; α,β-meATP

**Abbreviations:** α,β-meATP, α,β-methylene adenosine triphosphate; TNP-ATP, 2′,3′-O-(2,4,6,trinitrophenyl)-adenosine triphosphate

## Introduction

The $P2X_3$ receptor is an ATP-sensitive ligand-gated ion channel that is highly expressed on sensory afferent neurons (Chen *et al*., 1995; Lewis *et al*., 1995; Vulchanova *et al*., 1997). The selective localization of $P2X_3$ receptors on sensory neurons has generated considerable interest in the role of this receptor in the propagation of pain signaling (Burnstock, 2000; Jarvis & Kowaluk, 2001). The $P2X_3$ receptor is natively expressed as a functional homomer and also as a hetero-multimeric combination with the slowly desensitizing $P2X_2$ receptor ($P2X_{2/3}$ receptors) (Chen *et al*., 1995; Lewis *et al*., 1995; Lynch *et al*., 1999). These $P2X_3$ and $P2X_{2/3}$ receptors share highly similar pharmacological profiles (North, 2002), but differ in their acute desensitization kinetics (Collo *et al*., 1996; Lewis *et al*., 1995; Burgard *et al*., 1999). Consequently, activation of the heteromeric $P2X_{2/3}$ receptors can be pharmacologically distinguished from $P2X_2$ receptor-mediated responses, since it is sensitive to low concentrations of the $P2X_3$ agonist α,β-meATP, whereas the $P2X_2$ receptor is not (Collo *et al*., 1996; Lewis *et al*., 1995; Bianchi *et al*., 1999; Lynch *et al*., 1999).

Characterization of P2X receptor pharmacology has been hindered by the general lack of high-affinity ligands that selectively interact with specific P2X receptor subtypes (Jacobson *et al*., 2002). Antagonists such as suramin, PPADS, and reactive blue 2 have been traditionally used as P2X receptor antagonists (Jacobson *et al*., 2002). However, these compounds are relatively nonselective and have low micromolar affinity for P2X receptors (Bianchi *et al*., 1999). The ATP analog, 2′,3′-*O*-(2,4,6-trinitrophenyl)-ATP (TNP-ATP), has long been used as a probe for ATP binding sites (Mockett *et al*., 1994) and was later shown to be an antagonist of native P2X receptors (King *et al*., 1997). Subsequently, it was demonstrated that TNP-ATP had nanomolar affinity for blocking $P2X_1$, $P2X_3$, and $P2X_{2/3}$ receptors (Lewis *et al*., 1998; Thomas *et al*., 1998; Virginio *et al*., 1998). Recent investigation of the kinetics of receptor block by suramin, PPADS, and TNP-ATP has indicated that these compounds differ significantly in their respective rates of receptor association and dissociation, and that these differences contribute greatly to

*Author for corresponding; E-mail: michael.jarvis@abbott.com
[2]Current address: Dynogen Pharmaceuticals, Inc., Durham, NC 27709, U.S.A.
Advance online publication: 29 July 2003

their affinity for blocking the $P2X_{2/3}$ receptor (Spelta *et al*., 2002). In addition to these antagonists, a structurally novel non-nucleotide $P2X_3$ receptor antagonist, A-317491, has been reported, which has a high degree of potency and selectivity for $P2X_3$-containing channels as compared to its activity at other P2X receptors (Jarvis *et al*., 2002).

Agonist-induced fast desensitization of homomeric $P2X_3$ receptors also complicates the pharmacological analysis of these receptors. For example, TNP-ATP was originally reported to be a noncompetitive blocker of homomeric $P2X_3$ receptors (Virginio *et al*., 1998). However, analysis of the blockade of nondesensitizing ATP responses on cochlear hair cells (Mockett *et al*., 1994) and on recombinant human $P2X_{2/3}$ receptors (Burgard *et al*., 2000) provided evidence that TNP-ATP functions as a competitive antagonist. This apparent discrepancy may be related to the fact that the relatively slow off-rate of TNP-ATP from $P2X_3$ receptors can mask competitive inhibition over time due to the fast desensitization rate of this receptor (Burgard *et al*., 2000). As noted above, conclusive proof of this hypothesis has been difficult to obtain using the slowly desensitizing heteromeric $P2X_{2/3}$ receptor, because the $P2X_3$ selective agonist, $\alpha,\beta$-meATP, can activate $P2X_2$ receptors at high ($>100\,\mu$M) concentrations (Spelta *et al*., 2002), thus obscuring direct measurement of only the heteromeric receptor.

In an attempt to further address the issue of competitive antagonism of $P2X_3$ receptors, we have examined the ability of TNP-ATP and A-317491 (Figure 1) to block a chimeric human $P2X_{2-3}$ receptor that exhibits the acute slow-desensitization kinetics of the human $P2X_{2a}$ receptor (Lynch *et al*., 1999), while maintaining the pharmacological properties of the $P2X_3$ receptor. It has previously been shown through construction of chimeric $P2X_1$ and $P2X_2$ receptors that the two membrane-spanning domains (TMD1 and 2) are responsible for different rates of desensitization among these P2X receptor subunits (Werner *et al*., 1996). In addition, the first membrane-spanning domain has been shown to contribute to receptor gating and modulation of agonist affinity for the $P2X_2$ receptor (Haines *et al*., 2001). In the present studies, we have created a pair of chimeric human receptors between $P2X_{2a}$ and $P2X_3$ in which the N-terminal domain and TMD1 of one receptor were replaced with the analogous region of the other receptor. This exchange included the initial 41 amino acids of the $P2X_3$ receptor and the first 59 amino acids of the $P2X_{2a}$ receptor (Figure 2). To differentiate these chimeras from the heteromeric $P2X_{2/3}$ receptor, we refer to them as $P2X_{2-3}$ and $P2X_{3-2}$ (the first half being the N-terminal portion added and the second half being the original receptor host).

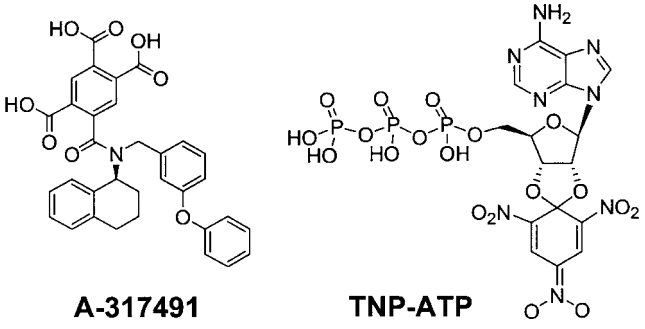


**Figure 1** Chemical structures of A-317419 and TNP-ATP.

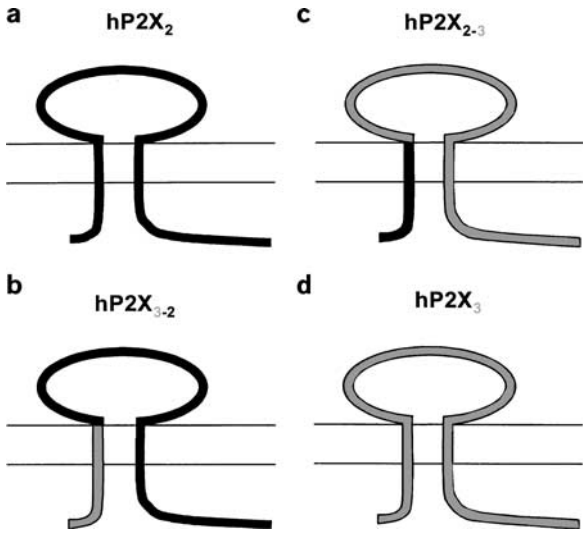


**Figure 2** Schematic of the native and chimeric P2X receptors.

## Methods

### *Human chimeric receptor construction*

The $hP2X_{2-3}$ chimeric receptor cDNA was created by substituting the coding sequence for the amino terminal 41 amino acids of the human $P2X_3$ receptor with the analogous region of the human $P2X_{2a}$ receptor (59 amino acids). Making the analogous switch into $P2X_2$ receptor created the $hP2X_{3-2}$ chimera. This was accomplished through the use of sequential overlap-PCR reactions. The first reaction utilized the parent P2X cDNAs as templates. For the $hP2X_{2-3}$ chimera, in one reaction, the human $P2X2_{2a}$ template cDNA was combined with a sense primer directed to the region surrounding the initiation codon of $P2X_{2a}$ and an antisense primer (5′AGC CTTCTCGTGCAAGAAAACGTACCACACGAAGTAGA GCAG3′). The other reaction employed the human $P2X_3$ cDNA as a template with an antisense primer directed to the region around the termination codon of $P2X_3$ and a chimeric sense primer (5′CTGCTCTACTTCGTGTGGTACGTTTT CTTGCACGAGAAGGCT3′). For the $hP2X_{3-2}$ chimera, in one reaction, the human $P2X_3$ template cDNA was combined with a sense primer directed to the region surrounding the initiation codon of $P2X_3$ and an antisense primer (5′GCTT TTCTGCACGATGAATACCCACCCTACAAAGTAGGA GAT3′). The other reaction employed the human $P2X_{2a}$ cDNA as a template with an antisense primer directed to the region around the termination codon of $P2X_{2a}$ and a chimeric sense primer (5′ATCTCCTACTTTGTAGGGTGGGTATT CATCGTGCAGAAAAGC3′). The amplification consisted of 2 min at 95°C, followed by 15 cycles of 94°C 20 s, 49°C 20 s, and 68°C 1 min. Products of these reactions were isolated *via* agarose gel electrophoresis and used as templates for a second round of amplification. The 5′ $P2X_{2a}$ initiation primer and 3′ $P2X_3$ termination primer were used in this reaction. Amplification conditions were as follows: 2 min at 94°C, five cycles of 94°C 30 s, 62°C 20 s, 68°C 90 s, and then 15 additional cycles of 94°C 20 s, 55°C 20 s, and 68°C 90 s Platinum *Pfx* DNA polymerase and buffers (Life Technologies, Inc.) were used for the amplifications. The amplification product was isolated *via* gel electrophoresis and cloned into pCRtopo 2.1 vector

(Invitrogen). The cDNA for the chimeric receptor was then transferred into the pIRESneo (Clontech) vector for generation of stable cell lines. The human $P2X_{2a}$ and $P2X_3$ receptors were cloned as described in Lynch *et al*. (1999). All data were obtained from human P2X receptors and all chimeric cDNAs were confirmed by sequence analysis using previously described methods (Lynch *et al*., 1999).

### *Stable cell line construction and culturing*

An expression plasmid encoding the human chimeric receptors was independently transfected into 1321N1 astrocytoma cells using Lipofectamine (Invitrogen, Carlsbad, CA, U.S.A.). Subsequently, stable clones of each receptor were selected using G418 ($800\,\mu g\,ml^{-1}$) and grown in culture as previously described (Bianchi *et al*., 1999; Burgard *et al*., 1999; Lynch *et al*., 1999). Cells were then maintained at 37°C in Dulbecco's modified Eagle's medium (DMEM) containing $4.5\,mg\,ml^{-1}$ glucose and 4 mM L-glutamine, 10% fetal bovine serum, and $300\,\mu g\,ml^{-1}$ G418. Stable human $P2X_3$ and $P2X_{2a}$ cell lines were constructed similarly.

### *Electrophysiology*

For patch-clamp recordings, 1321N1 cells were maintained in an extracellular recording solution (pH 7.4,. 325 mOsm) consisting of (mM): 155 NaCl, 5 KCl, 2 $CaCl_2$, 1 $MgCl_2$, 10 HEPES, 12 glucose. Patch pipettes (3–8 MΩ), composed of borosilicate glass, were pulled using a Flaming-Brown P87 micropipette puller (Sutter Instrument Co., San Rafael, CA, U.S.A.). Pipettes were then fire polished using a microforge (Narishige, Tokyo, Japan) and filled with internal solution (pH 7.3, 295 mOsm) consisting of (mM): 140 K-aspartate, 20 NaCl, 10 EGTA, 5 HEPES. Whole-cell recording techniques (Hamill *et al*., 1981) were utilized to voltage-clamp 1321N1 cells expressing recombinant P2X receptors at −60 mV using an Axopatch 200B amplifier (Axon Instruments, Foster City, CA, U.S.A.). Drugs were applied for 5–15 s at 2–5 min intervals to individual cells voltage-clamped at −60 mV (unless otherwise stated) using a piezo-electric-driven glass theta tube positioned close to the cell as previously described (Burgard *et al*., 2000). Increasing concentrations of agonist were applied to individual cells to generate concentration–response curves. Data acquisition and analysis were performed using pCLAMP 8.02 (Axon Instruments).

### *Pharmacology*

Pharmacological responses were measured using calcium-imaging techniques as previously described (Bianchi *et al*., 1999; Burgard *et al*., 2000). Fluo-4, a fluorescent $Ca^{2+}$-chelating dye, was used as an indicator of the relative levels of intracellular $Ca^{2+}$ in a 96-well format with a Fluorescence Imaging Plate Reader (FLIPR, Molecular Devices). Cells expressing recombinant human P2X receptors were grown to confluence and plated in 96-well black-walled tissue culture plates approximately 18 h prior to the experiment. At 1–2 h before the assay, cells were loaded with fluo-4 AM (2.28 μM; Molecular Probes, Eugene, OR, U.S.A.) in D-PBS and maintained in a dark environment at room temperature. Immediately before the assay, each plate was washed twice with 250 μl D-PBS per well in order to remove extracellular fluo-4 AM. Two 50 μl additions of compounds (prepared in D-PBS) were made to the cells during each experiment. The first compound addition (antagonist or vehicle control) was made and incubation continued for the remainder of the experiment. The second compound addition (test P2X receptor agonist) occurred 3 min after the first and measurement continued for 3 min after this final addition. Data shown are based on the average peak increase in relative fluorescence units, as compared to basal fluorescence for the population of cells from multiple wells treated with a single agonist or antagonist concentration on each coverslip. Concentration–response curves and Schild plots were generated by taking these average values and plotting them as a function of the concentration of the drug. Therefore, with this technique, cells were only exposed to agonist one time, thus removing potential confounding effects of progressive desensitization that may be present in the electrophysiological experiments.

### *Data analysis*

Agonist concentration–response curves were fitted by least-squares regression to the logistic equation:

$$Y = \min + [(\max - \min)/(1 + 10^{((\log EC_{50} - X)n_H)})]$$

where $Y$, min, and max represent the measured minimum and maximum responses respectively; $EC_{50}$ is the ligand concentration giving half-maximal response; $X$ is the concentration of ligand used, and $n_H$ is the Hill coefficient. Graphs and curve fits were generated using Prism (Graphpad Software, San Diego, CA, U.S.A.).

Competitive inhibition was determined using Schild analysis (Arunlakshana & Schild, 1959). $pA_2$ values were determined from a least-squares linear regression fitted to the Schild plots using Prism (Graphpad Software, San Diego, CA, U.S.A.).

All reagents were obtained from Sigma Chemical Co. (St Louis, MO, U.S.A.) except A-317491 (synthesized at Abbott Laboratories, Abbott Park, IL, U.S.A.) and TNP-ATP and Fluo-4 (Molecular Probes, Eugene, OR, U.S.A.).

## Results

### *Biophysical and pharmacological properties of chimeric receptors*

Chimeric receptors stably transfected into 1321N1 astrocytoma cells were initially characterized using whole-cell patch-clamp electrophysiological techniques. Individual 1321N1 cells expressing the chimeric receptors were voltage clamped at potentials ranging from −100 to + 60 mV at 20 mV increments and the average peak whole-cell currents were plotted as a function of these holding potentials. The chimeric $P2X_{2-3}$ and $P2X_{3-2}$ receptors, similar to the wild-type receptors, showed pronounced inward rectification (Figure 3a,b). For comparison, we show that $P2X_{2a}$ and $P2X_3$ receptors expressed in 1321N1 cells also have inwardly rectifying current–voltage relations (Figure 3c,d), similar to what has previously been shown in oocytes (Lynch *et al*., 1999). These results indicate that this biophysical feature of the channel was not disrupted by the formation of the chimeric receptors.

The application of ATP (30 nM–30 μM) to cells expressing the $P2X_{2-3}$ chimera produced a concentration-dependent

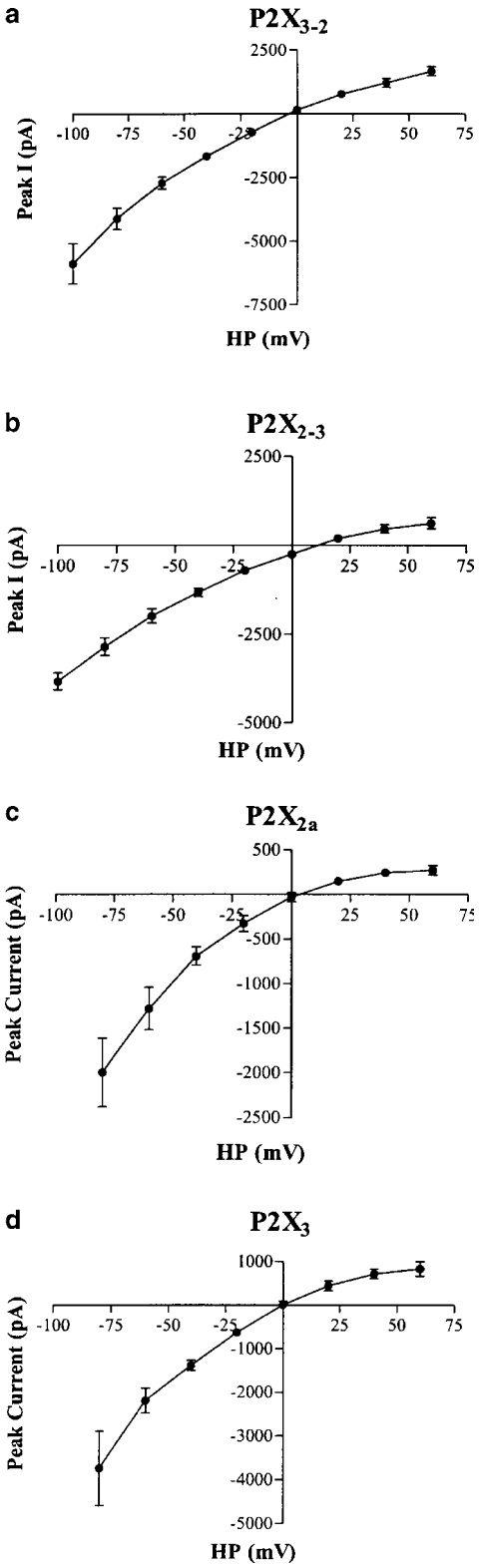


**Figure 3** Current–voltage relationships of agonist-activated responses in cells expressing P2X receptors. Inwardly rectifying current–voltage curves were observed in both native and chimeric P2X receptors (a–d). Current–voltage curves are shown where the average peak currents evoked by agonist were plotted as a function of the membrane-holding potential (−80 to +60 mV) ($P2X_{2-3}$: 10 $\mu$M $\alpha,\beta$-meATP; $P2X_2$, $P2X_{3-2}$: 10 $\mu$M ATP; $P2X_3$: 3 $\mu$M ATP). Chimeric and wild-type receptors were stably expressed in 1321N1 cells and currents were recorded using whole-cell patch-clamp techniques (a–d). Data are mean ± s.e.m.

increase in current amplitude with maximal currents reaching 1733 ± 415 pA at 30 $\mu$M. Normalized peak currents were averaged, plotted as a function of ATP concentration, and fit with a sigmoidal logistic equation with an $EC_{50}$ of 327 nM (Figure 4a, Table 1). Cells expressing the $P2X_{3-2}$ chimera also had concentration-dependent currents evoked by ATP with maximal peak currents reaching 2003 ± 279 pA. Fits of the averaged normalized data resulted in an $EC_{50}$ = 970 nM (Figure 4a). Concentration–response curves for wild-type $P2X_2$ ($EC_{50}$ = 7.4 $\mu$M) and $P2X_3$ ($EC_{50}$ = 130 nM) receptors (Figure 3a, dashed lines, Table 1) are shown for comparison.

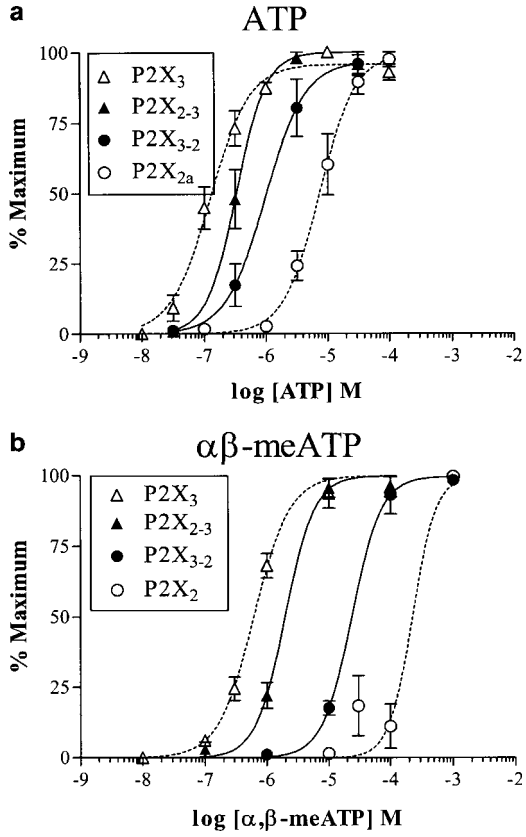


**Figure 4** Agonist concentration–response curves for wild-type and chimeric P2X receptors. (a) ATP (30 nM–1 mM) stably expressed in 1321 cells. (b) $\alpha,\beta$-meATP (100 nM–1 mM). Current amplitudes are expressed as a percentage of the maximum (% maximum) response for each agonist. Data are mean ± s.e.m.

**Table 1** Electrophysiological characterization of chimeric and wild-type P2X receptor pharmacology

| | *ATP* | | *α,β-meATP* | |
|---|---|---|---|---|
| | $EC_{50}$ (μM) | $n_H$ | $EC_{50}$ (μM) | $n_H$ |
| $P2X_3$ | 0.13 ± 0.06 | 1.4 ± 0.22 | 0.62 ± 0.03 | 1.5 ± 0.15 |
| $P2X_{2-3}$ | 0.33 ± 0.03 | 1.8 ± 0.62 | 1.97 ± 0.06 | 1.8 ± 0.31 |
| $P2X_{3-2}$ | 0.97 ± 0.01 | 1.3 ± 0.01 | 23.4 ± 0.02 | 1.8 ± 0.07 |
| $P2X_2$ | 7.36 ± 0.03 | 1.5 ± 0.11 | > 300 | > 2 |

Each value represents the best fit of a logistic equation to the averaged data from concentration–response curves from three to six cells. Values are mean $EC_{50}$ ± s.e.m. (standard error of the mean); $n_H$ = Hill slope.

A concentration-dependent activation of the chimeric receptors was also produced by α,β-meATP (100 nM–100 μM). Maximal currents of 1270±249 pA at 100 μM α,β-meATP were recorded from $P2X_{2-3}$-expressing cells. Fits of the averaged normalized α,β-meATP data resulted in an $EC_{50}$ of 1.97 μM (Figure 4b, Table 1). A similar concentration-dependent effect of α,β-meATP ($EC_{50}=23\,\mu M$) was seen in cells expressing $P2X_{3-2}$ receptors with maximal currents of 1728±893 pA at 100 μM (Figure 4b). The concentration-dependent responses of wild-type $P2X_3$ are shown for comparison ($EC_{50}=0.62\,\mu M$). $P2X_2$ wild-type receptors were insensitive to α,β-meATP up to 300 μM and at 1 mM small currents of only 536±147 pA were activated (Figure 4b). These currents were significantly smaller than that of either chimeric receptor or the wild-type $P2X_3$ receptor. For comparison, normalized currents were plotted as a function of α,β-meATP concentration and fit with a logistic equation. However, since the responses did not reach a plateau level, it can only be concluded that the $EC_{50}$ of α,β-meATP is greater than 300 μM for these channels.

In the course of these patch-clamp experiments, it was evident that the kinetics of desensitization of the $P2X_{2-3}$ chimeric receptor was more similar to the $P2X_{2a}$ receptor than to the $P2X_3$ receptor. Likewise, the reverse chimera, $P2X_{3-2}$, showed a faster desensitizing component as compared to the $P2X_2$ receptor. Figure 5 illustrates the differences in desensitization kinetics in response to near-maximal concentrations of ATP applied for 16 s (3 μM for $P2X_3$ and $P2X_{2-3}$ chimeric receptors, 30 μM for the $P2X_{3-2}$ chimeric receptors and 100 μM for the less sensitive $P2X_{2a}$ receptor).

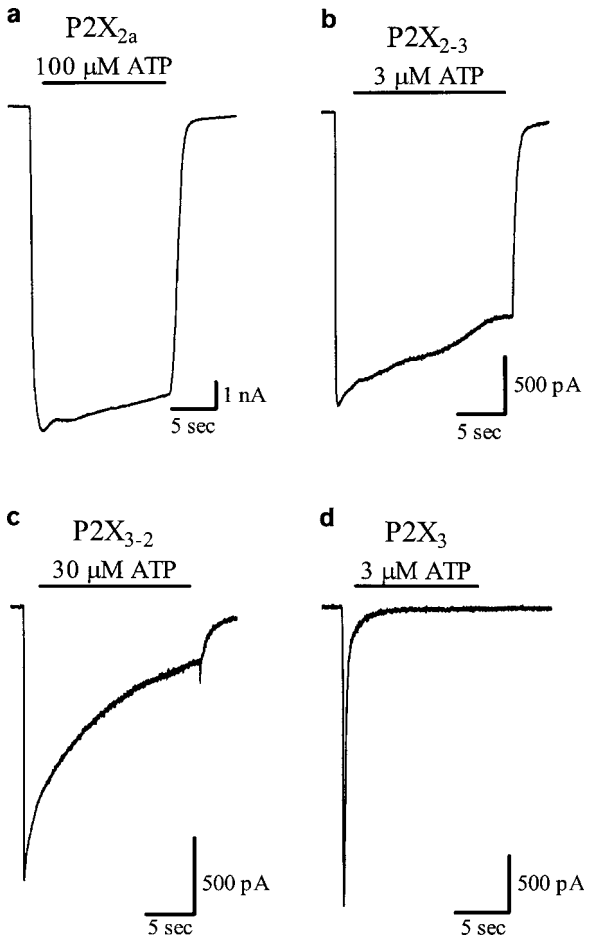


**Figure 5** Altered desensitization kinetics of human P2X chimeric receptors. Cells were voltage-clamped at −60 mV and maximal concentrations of ATP (3, 30 or 100 μM) were applied for 16 s (denoted by bar). Representative inward currents recorded from cells expressing P2X receptors are shown, illustrating that replacing the N-terminal portion of the rapidly desensitizing $P2X_3$ receptor (d) with the slowly desensitizing $P2X_{2a}$ receptor (a), results in a chimeric receptor with slowly desensitizing currents (b). In addition, making the analogous chimera (replacing the N-terminal domain of the $P2X_2$ receptor with that of $P2X_3$), results in a receptor with faster desensitizing currents (c). Wild-type and chimeric channel currents were recorded from stably transfected 1321N1 cells using whole-cell patch-clamp techniques.

### *Pharmacological profile of chimeric receptor using fluorescence-based assay*

In parallel with the electrophysiological characterization of the chimeric receptor, we investigated the kinetics and pharmacology of the receptor using calcium-imaging techniques. 1321N1 cells stably expressing the chimeric $P2X_{2-3}$ receptor were loaded with Fluo-4, a fluorescent calcium dye, and challenged with 3 μM ATP. Like the electrophysiological results, the chimeric $P2X_{2-3}$ receptor did not show the agonist-induced fast-desensitization kinetics seen in the $P2X_3$ wild-type receptors, whereas the $P2X_{3-2}$ chimeras did show increased acute receptor desensitization (Figure 6). The extent and apparent rate of desensitization were similar to the receptor that contributed the N-terminal portion to the chimeric receptor.

Concentration–response curves were generated for ATP and α,β-meATP at the wild-type $P2X_{2a}$ and $P2X_3$ receptors and the chimeric receptors using the calcium influx assay. ATP (10 nM–100 μM) produced concentration-dependent responses at all four receptor subtypes. Both chimeric receptors had steep concentration-dependent responses in response to ATP with maximum fluorescence signals achieved at 1 μM and $EC_{50}$'s around 250 nM (Figure 7a, Table 2). Similar to the chimeric receptors, ATP showed high affinity for the $P2X_3$ receptor ($EC_{50}=400$ nM). In contrast, $P2X_{2a}$ receptors had an $EC_{50}$ for ATP of 1.07 μM (Figure 7a, Table 2). Thus, calcium imaging and electrophysiology produced similar measures of agonist sensitivity at both wild-type ($P2X_2$ and $P2X_3$) and chimeric ($P2X_{2-3}$ and $P2X_{3-2}$) receptors.

Concentration-dependent responses were also evoked by application of α,β-meATP (1 nM-100 μM) in cells expressing the chimeric and native $P2X_3$ receptors. Maximum responses for both $P2X_3$ and the chimeric $P2X_{2-3}$ receptors were evoked by application of 10 μM α,β-meATP (Figure 7b). In contrast, the $P2X_{3-2}$ required much higher concentrations of α,β-meATP to reach maximal responses (~100 μM). The calculated $EC_{50}$ for the chimeric $P2X_{2-3}$ receptor was similar to that of the $P2X_3$ receptor, but significantly less than the $P2X_{3-2}$ chimera (Table 2). At the $P2X_{2a}$ receptor, α,β-meATP did not produce any significant response until 100 μM. This resulted in a steep concentration–response curve that did not plateau, similar to the electrophysiological results. A fit of the normalized data resulted in a calculated $EC_{50}$ of 43.4 μM with an extremely high Hill slope (9.7). However, since no upper plateau was reached, all that can be concluded from these data are that the $EC_{50}$ for α,β-meATP is greater than 30 μM at the $P2X_{2a}$ receptor.

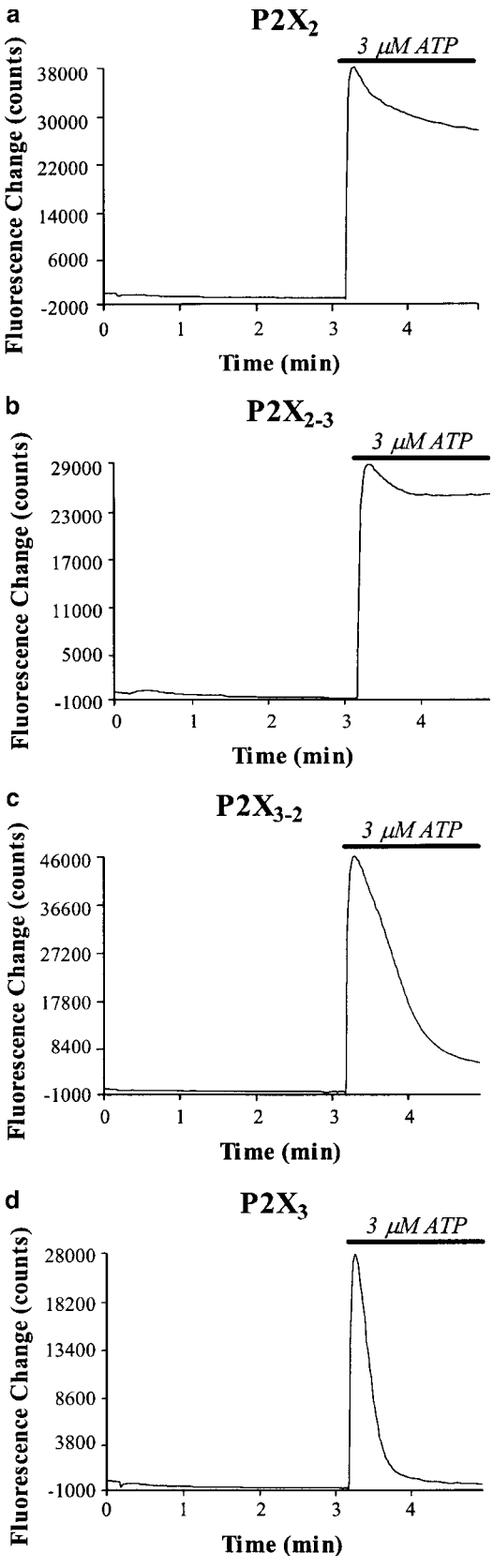


**Figure 6** Kinetics of ATP-activated $Ca^{2+}$ influx in 1321N1 cells expressing P2X receptor subtypes. Changes in Fluo-4 fluorescence were measured in response to application of 3 $\mu$M ATP (denoted by bars). These are raw FLIPR traces obtained from individual experimental runs and show that the kinetics of the P2X channel responses is similar to that recorded using patch-clamp techniques.

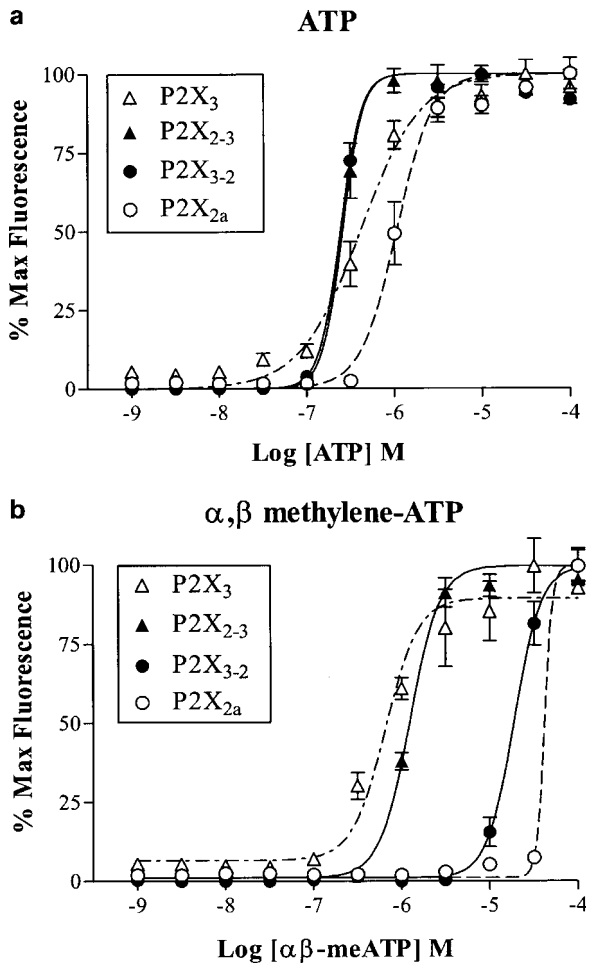


**Figure 7** Effect of concentration on agonist-activated $Ca^{2+}$ influx for wild-type and chimeric P2X receptors. The chimeric receptors have agonist pharmacology similar to the native receptor contributing the extracellular domains. Agonist concentration–response curves obtained from four different P2X receptors to ATP (a) and $\alpha,\beta$-meATP (b). In these calcium-imaging experiments, values were normalized to peak Fluo-4 fluorescence intensities obtained in the presence of agonist. Each curve represents the mean $\pm$ s.e.m. for two to six experiments under each condition.

Concentration-dependent effects of other P2X receptors agonists (BzATP, ADP, ATP$\gamma$S, 2-meS-ATP) were also tested on the two wild-type receptors and chimeric receptors, and the results are summarized in Table 2. In each case, the affinity of the agonist at the $P2X_{2-3}$ chimeric receptor was similar to that obtained at the $P2X_3$ receptor ($EC_{50}$'s were generally one- to four-fold apart), and significantly different from the $P2X_{2a}$ receptor (generally greater than five-fold different). One exception to this trend was ATP$\gamma$S which was relatively insensitive at the $P2X_{2-3}$ chimeric receptor compared to both wild-type receptors.

To address whether TNP-ATP is a competitive or non-competitive antagonist, a Schild analysis was performed on cells expressing the $P2X_{2-3}$ receptor. Concentration–response curves were generated for ATP (100 nM–30 $\mu$M) using the calcium influx assay in the presence of increasing concentrations of TNP-ATP (0.6–40 nM). Peak ATP responses were plotted as a function of ATP concentration and fitted with logistic equations in the presence of increasing TNP-ATP concentrations (Figure 8a). The resulting $EC_{50}$'s were then

**Table 2** Calcium-imaging experiments characterizing the pharmacology of chimeric and wild-type P2X receptors

| | *ATP* $EC_{50}$ ($\mu$M) | *α,β-meATP* $EC_{50}$ ($\mu$M) | *ATPγS* $EC_{50}$ ($\mu$M) | *BzATP* $EC_{50}$ ($\mu$M) | *2-meS-ATP* $EC_{50}$ ($\mu$M) | *ADP* $EC_{50}$ ($\mu$M) |
|---|---|---|---|---|---|---|
| $P2X_3$ | 0.40±0.03 | 0.78±0.08 | 0.55±0.04 | 0.04±0.03 | 0.18±0.04 | 15.00±1.27 |
| $P2X_{2-3}$ | 0.27±0.02 | 1.21±0.11 | 4.35±0.48 | 0.01±0.004 | 0.04±0.004 | 15.27±2.54 |
| $P2X_{3-2}$ | 0.24±0.02 | 18.84±2.49 | 0.36±0.06 | 0.31±0.09 | 0.29±0.05 | 32.19±0.60 |
| $P2X_2$ | 1.07±0.13 | >30 | 0.88±0.04 | 1.05±0.32 | 0.56±0.03 | >100 |

Each value represents the mean $EC_{50}$±s.e.m. values ($\mu$M) calculated from 2 to 16 concentration–response curves run in duplicate.

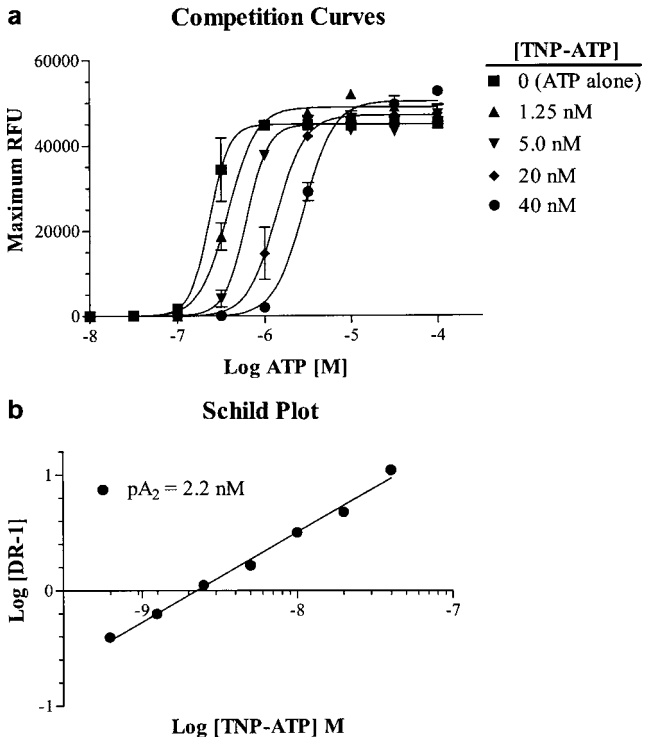


**Figure 8** TNP-ATP is a competitive antagonist of human P2X2-3 chimeric receptor. Agonist concentration curves for ATP were generated in the presence of increasing ($n=7$) concentrations (0.5–40 nM) of TNP-ATP. (a) Shown are selected curves from the range tested, illustrating the rightward shift and full efficacy of the ATP concentration–response curves. Some intermediate concentrations were removed for clarity. (b) Schild plot of all the competition curve data reveals a linear relationship with slope = 1.3 and $pA_2 = 2.2$ nM.

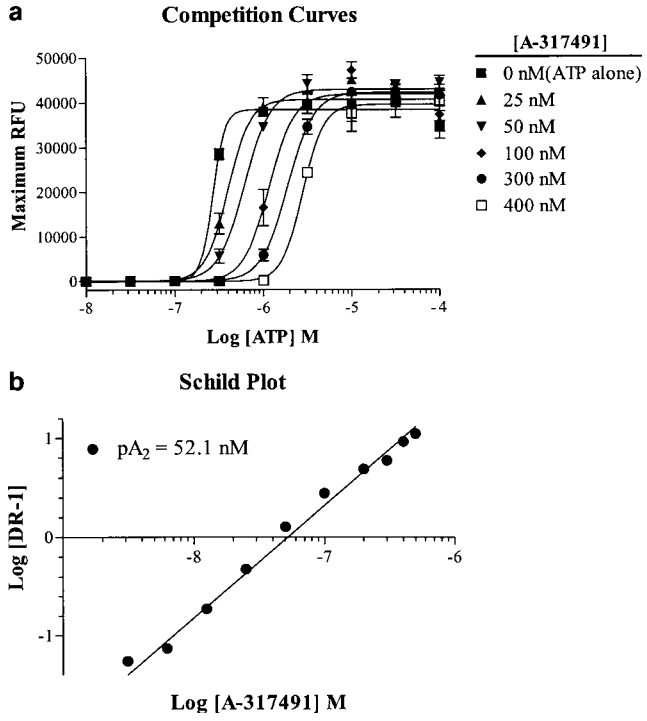


**Figure 9** The novel non-nucleotide compound, A-317491, is a competitive antagonist at the $P2X_{2-3}$ chimeric receptor. Competition curves for ATP generated in the presence of increasing ($n=10$) concentrations (12.5–500 nM) of A-317491. (a) Selected curves from the range tested illustrating the rightward shift and full efficacy of the ATP concentration–response curves are shown. Some intermediate concentrations were removed for clarity. (b) Schild plot of all the competition curve data reveals a linear relationship with slope = 1.1 and $pA_2 = 52.1$ nM.

plotted in relation to the concentration of TNP-ATP present. As predicted for a competitive antagonist, TNP-ATP produced a linear rightward shift in the ATP concentration–response curve, which was fitted with a linear regression resulting in a $pA_2$ value of 2.2 nM with a slope of 1.3 (Figure 8b).

Concentration–response curves were generated for ATP (100 nM–30 $\mu$M) in the presence of increasing concentrations of the novel P2X antagonist A-317491 (12.5–500 nM) in 1321N1 cells expressing the $P2X_{2-3}$ receptor (Figure 9a). Similar to TNP-ATP, a rightward shift in the ATP concentration–response curve was observed, which resulted in a linear Schild plot with a slope of 0.9 and a $pA_2$ of 52.1 nM (Figure 9b). In addition, A-317491 was virtually inactive at the $P2X_{3-2}$ chimeric and showed no concentration-dependent shifts in a competition experiment (data not shown) consistent with $P2X_{3-2}$ having a pharmacological profile similar to $P2X_2$.

## Discussion

The present studies were undertaken to further characterize the nature of the antagonist block of the $P2X_3$-containing channels. Previous work from our lab had shown that the relatively slow-off kinetics of the potent antagonist, TNP-ATP, could potentially obscure the competitive antagonism at the fast-desensitizing homomeric $P2X_3$ receptor (Burgard *et al.*, 2000). Analysis of the heteromeric $P2X_{2/3}$ receptor, while overcoming the fast-desensitization properties of the homomeric channel, is complicated by the presence of homomeric $P2X_3$ and $P2X_2$ receptors that can coexist with $P2X_{2/3}$ receptors in stably transfected mammalian cells created to express $P2X_{2/3}$ heteromeric receptors. α,β-meATP shows similar potency to activate both homomeric and heteromeric $P2X_3$-containing channels and is a relatively poor agonist for the $P2X_2$ receptor. However, Spelta *et al.* (2002) have recently

demonstrated that α,β-meATP can effectively activate $P2X_2$ receptors at high (>100 μM) concentrations. This complication in the pharmacological analysis of the pharmacology of the $P2X_{2/3}$ receptor may also be dependent on mammalian species homologue (rat vs human) and the method of stable receptor transfection (Jarvis & Burgard, 2002).

Previously, Werner *et al*. (1996) showed that substituting transmembrane and intracellular domains of $P2X_2$ receptors could markedly reduce agonist-induced receptor desensitization of the fast-desensitizing $P2X_1$ receptor. We adopted a similar strategy and created chimeras between $P2X_3$ and $P2X_2$ receptors to resolve the mode of action of receptor antagonists such as TNP-ATP and A-317491. These chimeric receptors eliminate the potential complications of both coexpression of multiple channel isoforms and of rapid receptor desensitization.

The pharmacological analysis of the $P2X_3$ chimeric receptors indicated that responses to receptor antagonists were very similar to the wild-type channel contributing the extracellular domain of the chimera. In addition, the agonist pharmacology of the chimeric $P2X_{2-3}$ receptor matches well with that of the wild-type $P2X_3$ receptor, whereas the $P2X_{3-2}$ chimera agonist profile was intermediate between what we have previously observed for the $P2X_2$ and $P2X_3$ receptors (Bianchi *et al*., 1999; Lynch *et al*., 1999).

The pharmacological and desensitization properties of the $P2X_{2-3}$ chimeras make them uniquely suitable to address the mode of action of antagonists such as TNP-ATP. While TNP-ATP had originally been characterized as a low-affinity, but competitive, antagonist of endogenous P2X receptors (Mockett *et al*., 1994; King *et al*., 1997), more recent studies had discovered that TNP-ATP was a potent (nM) antagonist of $P2X_3$- and $P2X_1$-containing channels (Lewis *et al*., 1998; Virginio *et al*., 1998). We demonstrated that TNP-ATP blocked agonist activation of recombinant heteromeric $P2X_{2/3}$ receptors in an apparent competitive fashion and provided evidence suggesting that the rapidly desensitizing $P2X_3$ currents masked the competitive antagonism of TNP-ATP (Burgard *et al*., 2000). This high-affinity antagonism is determined by the ultra-fast association rate of TNP-ATP (~50-fold faster than other antagonists) and not its dissociation rate (Spelta *et al*., 2002), as we had originally concluded (Burgard *et al*., 2000). The present data demonstrated that TNP-ATP produced a concentration-dependent parallel rightward shift in the effect of ATP at the chimeric $P2X_{2-3}$ receptor without altering the peak response, consistent with competitive antagonism. Additionally, A-317491, a novel potent and selective non-nucleotide antagonist of $P2X_3$-containing channels, was also shown to competitively block chimeric $P2X_{2-3}$ responses consistent with its competitive activity at the heteromeric $P2X_{2/3}$ receptor (Jarvis *et al*., 2002). The potencies of both TNP-ATP and A-317491 to block the chimeric $P2X_{2-3}$ receptor were similar to what we had previously reported for the heteromeric $P2X_{2/3}$ channel ($pA_2$ values of 2.2 vs 2.0 nM for TNP-ATP and 52.1 vs 232 nM for A-317491) (Burgard *et al*., 2000; Jarvis *et al*., 2002). In addition, A-317491 exhibited similar on and off rate constants (unpublished observations) as compared to TNP-ATP (Burgard *et al*., 2000).

Formation of chimeric receptors was accomplished by swapping the N-terminal domain and first transmembrane domain (TMD) of either human $P2X_2$ or $P2X_3$ subunits and attaching them to the extracellular, TMD2, and C-terminal portion of the other channel. Expression of these chimeras resulted in functional receptors with desensitization kinetics similar to their respective native receptors that contributed the N-terminal domain. The degree of desensitization for the $P2X_{2-3}$ chimeric receptor was significantly faster than that of native $P2X_2$ receptors but not quite as fast as native $P2X_3$ receptors. Similarly, the chimeric $P2X_{3-2}$ receptor had dramatically slower desensitization kinetics as compared to the $P2X_3$ receptor, but not as slow as the native $P2X_2$ receptor. These desensitization properties were apparent in both whole-cell patch-clamp electrophysiological measurements as well as calcium-imaging experiments. The desensitization kinetics of the chimeric $P2X_{2-3}$ and $P2X_{3-2}$ receptors is in agreement with similar data reported for chimeric $P2X_1$ and $P2X_2$ receptors by Werner *et al*. (1996). These investigators demonstrated that switching out one TMD was sufficient to reduce the desensitization kinetics of native $P2X_1$ receptors, but that switching both TMDs were required to impart strong or total desensitization kinetics on $P2X_2$ receptors (Werner *et al*., 1996). Conversely, they showed that removal of either TMD1 or 2 was sufficient to remove desensitization from $P2X_1$ receptors. The present chimeric receptors, however, involved more extensive modifications as they also included the N-terminal domain along with TMD1. Taken together, these results indicate that like $P2X_1$, the N-terminal portion (along with TMD1) of $P2X_3$ is sufficient to alter the rate of desensitization in slowly desensitizing P2X receptors.

Based on the pharmacology of the $P2X_{2-3}$ receptor, we would have predicted that the $P2X_{3-2}$ chimera would have a pharmacological profile similar to the wild-type $P2X_2$ receptor. However, the $P2X_{3-2}$ chimeric receptor often displayed an agonist pharmacology that was intermediate between the two wild-type receptors. This was particularly evident when comparing the relatively potent effect of α,β-meATP at the chimeric receptor, observed in both electrophysiological and calcium-imaging assays, to that at the α,β-meATP-insensitive $P2X_2$ receptors. Although the $P2X_{3-2}$ chimera showed some sensitivity to α,β-meATP, which differentiated it from $P2X_2$ receptors, it was significantly less potent when compared to its actions at the wild-type $P2X_3$ receptors or the $P2X_{2-3}$ chimera receptors. Interestingly, a chimera constructed by replacing the N-terminal portion of the extracellular domain ($Val^{60}$ to $Arg^{180}$) of $P2X_3$ with the analogous region of $P2X_2$ was sufficient to confer α,β-meATP sensitivity to the receptor (Koshimizu *et al*., 2002) but with $P2X_2$-like desensitization. These results suggest that alteration of the $P2X_2$ receptor to increase the rate of desensitization of the channel alters the apparent affinity of the agonist.

Recently, two other groups have created chimeric receptors between $P2X_2$ and $P2X_3$ in order to investigate the interactions of specific receptor domains in creating the desensitizing phenotype and receptor heteromultimerization (He *et al*., 2002; Koshimizu *et al*., 2002). In each case, both intracellular domains of the $P2X_3$ receptor were replaced with those of the $P2X_2$ receptor and the resulting chimeric receptors showed altered desensitization rates and agonist sensitivities analogous to the present data for the $P2X_{3-2}$ receptor.

The alteration of agonist pharmacology of the $P2X_{3-2}$ chimeric receptor, as compared to the wild-type $P2X_2$ receptor, necessarily limits a clear interpretation of the mode of antagonist block of this chimera. However, these data raise interesting questions concerning the contributions of different

regions of the receptor to agonist recognition/binding and the potential influence of channel kinetics on agonist pharmacology. As noted above, He *et al*. showed that there is a correlation between agonist affinity at the $P2X_2$ receptor and the degree of desensitization produced by the agonist. Furthermore, these investigators demonstrated that the construction of a chimeric receptor between $P2X_2$ and $P2X_7$ receptors reduced the receptor's sensitivity for ATP and blocked C-terminus-dependent desensitization of the chimera. The present data also show apparent shifts in agonist affinity for the $P2X_{3-2}$ chimera that correlate with the desensitization properties of the chimeric channel, thus providing evidence that the N-terminal portion of the channel may also contribute to this characteristic of P2X receptors.

In conclusion, our results demonstrate that TNP-ATP and the non-nucleotide antagonist, A-317491, competitively block agonist activation of the $P2X_3$-containing channels. These findings are consistent with previous reports that suggested this mechanism of action; however, the previous studies were necessarily limited by the lack of truly selective $P2X_3$ receptor agonists and by the ambiguity associated with the heterologous expression of multiple receptor subunits in the construction of the stably transfected $P2X_{2/3}$ receptor cell line.

## References


ARUNLAKSHANA, O. & SCHILD, H.O. (1959). Some quantitative uses of drug antagonists. *Brit J Pharmacol.,* **4,** 48–58.

BIANCHI, B.R., LYNCH, K.J., TOUMA, E., NIFORATOS, W., BURGARD, E.C., ALEXANDER, K.M., PARK, H.S., YU, H., METZGER, R., KOWALUK, E., JARVIS, M.F. & VAN BIESEN, T. (1999). Pharmacological characterization of recombinant human and rat P2X receptor subtypes. *Eur. J. Pharmacol.,* **376,** 127–138.

BURNSTOCK, G. (2000). P2X receptors in sensory neurones. *Br. J. Anaesth.,* **4,** 476–488.

BURGARD, E.C., NIFORATOS, W., VAN BIESEN, T., LYNCH, K.J., TOUMA, E., METZGER, R.E., KOWALUK, E.A. & JARVIS, M.F. (1999). P2X receptor-mediated ionic currents in dorsal root ganglion neurons. *J. Neurophysiol.,* **82,** 1590–1598.

BURGARD, E.C., NIFORATOS, W., VAN BIESEN, T., LYNCH, K.J., KAGE, K.L., TOUMA, E., KOWALUK, E.A. & JARVIS, M.F. (2000). Competitive antagonism of recombinant P2X(2/3) receptors by 2′, 3′-*O*-(2,4,6-trinitropnenyl) adenosine 5′-triphosphate (TNP-ATP). *Mol. Pharmacol.,* **58,** 1502–1510.

CHEN, C.C., AKOPIAN, A.N., SIVILOTTI, L., COLQUHOUN, D., BURNSTOCK, G. & WOOD, J.N. (1995). A P2X purinoceptor expressed by a subset of sensory neurons. *Nature,* **377,** 428–431.

COLLO, G., NORTH, R.A., KAWASHIMA, E., MERLO-PICH, E., NEIDHART, S., SURPRENANT, A. & BUELL, G. (1996). Cloning of $P2X_5$ and $P2X_6$ receptors and the distribution and properties of an extended family of ATP-gated ion channels. *J. Neurosci.,* **16,** 2495–2507.

HAINES, W.R., MIGITA, K., COX, J.A., EGAN, T.M. & VOIGT, M.M. (2001). The first transmembrane domain of the P2X receptor subunit participates in the agonist-induced gating of the channel. *J. Biol. Chem.,* **276,** 32793–32798.

HAMILL O.P. MARTY, A., NEHER, E., SAKMANN, B. & SIGWORTH, F.J. (1981). Improved patch-clamp techniques for high resolution current recordings from cells and cell-free membrane patches. *Pflugers Arch.,* **391,** 85–100.

HE, M.L., KOSHIMIZU, T.A., TOMIC, M. & STOJILKOVIC, S.S. (2002). Purinergic P2X(2) receptor desensitization depends on coupling between ectodomain and C-terminal domain. *Mol. Pharmacol.,* **62,** 1187–1197.

JACOBSON, K.A., JARVIS, M.F. & WILLIAMS, M. (2002). Perspective: purine and pyrimidine (P2) receptors as drug targets. *J. Med. Chem.,* **45,** 4057–4093.

JARVIS, M.F. & BURGARD, E.C. (2002). Antagonism of $P2X_3$-containing channels: commentary on Spelta *et al*. *Br. J. Pharmacol.,* **135,** 1343–1344.

JARVIS, M.F., BURGARD, E.C., MCGARAUGHTY, S., HONORE, P., LYNCH, K., BRENNAN, T.J., SUBIETA, A., VAN BIESEN, T., CARTMELL, J., BIANCHI, B., NIFORATOS, W., KAGE, K., YU, H., MIKUSA, J., WISMER, C.T., ZHU, C.Z., CHU, K., LEE, C.H., STEWART, A.O., POLAKOWSKI, J., COX, B.F., KOWALUK, E., WILLIAMS, M., SULLIVAN, J. & FALTYNEK, C. (2002). A-317491, a novel potent and selective non-nucleotide antagonist of $P2X_3$ and $P2X_{2/3}$ receptors, reduces chronic inflammatory and neuropathic pain in the rat. *Proc. Natl. Acad. Sci. U.S.A.,* **99,** 17179–17184.

JARVIS, M.F. & KOWALUK, E.A. (2001). Pharmacological characterization of $P2X_3$ homomeric and heteromeric channels in receptors nociceptive signaling and behavior. *Drug Dev. Res.,* **52,** 220–231.

KING, B.F., WILDMAN, S.S., ZIGANSHINA, L.E., PINTOR, J. & BURNSTOCK, G. (1997). Effects of extracellular pH on agonism and antagonism at a recombinant $P2X_2$ receptor. *Br. J. Pharmacol.,* **121,** 1445–1453.

KOSHIMIZU, T.A., UENO, S., TANOUE, A., YANAGIHARA, N., STOJILKOVIC, S.S. & TSUJIMOTO, G. (2002). Heteromultimerization modulates P2X receptor functions through participating extracellular and C-terminal subdomains. *J. Biol. Chem.,* **277,** 46891–46899.

LEWIS, C., NEIDHART, S., HOLY, C., NORTH, R.A., BUELL, G. & SURPRENANT, A. (1995). Coexpression of $P2X_2$ and $P2X_3$ receptor subunits can account for ATP-gated currents in sensory neurons. *Nature,* **377,** 432–435.

LEWIS, C.J., SURPRENANT, A. & EVANS, R.J. (1998). 2′,3′-*O*-(2,4,6-trinitrophenyl) adenosine 5′-triphosphate (TNP-ATP)–a nanomolar affinity antagonist at rat mesenteric artery P2X receptor ion channels. *Br. J. Pharmacol.,* **124,** 1463–1466.

LYNCH, K.J., TOUMA, E., NIFORATOS, W., KAGE, K.L., BURGARD, E.C., VAN BIESEN, T., KOWALUK, E.A. & JARVIS, M.F. (1999). Molecular and functional characterization of human P2X(2) receptors. *Mol. Pharmacol.,* **56,** 1171–1181.

MOCKETT, B.G., HOUSLEY, G.D. & THORNE, P.R. (1994). Fluorescence imaging of extracellular purinergic receptor sites and putative ecto-ATPase sites on isolated cochlear hair cells. *J. Neurosci.,* **14,** 6992–7007.

NORTH, R.A. (2002). Molecular physiology of P2X receptors. *Physiol. Rev.,* **82,** 1013–1067.

SPELTA, V., JIANG, L.H., SURPRENANT, A. & NORTH, R.A. (2002). Kinetics of antagonist actions at rat $P2X_{2/3}$ heteromeric receptors. *Br. J. Pharmacol.,* **135,** 1524–1530.

THOMAS, S., VIRGINIO, C., NORTH, R.A. & SURPRENANT, A. (1998). The antagonist trinitrophenyl-ATP reveals co-existence of distinct P2X receptor channels in rat nodose neurones. *J. Physiol.,* **509** (Part 2), 411–417.

VIRGINIO, C., ROBERTSON, G., SURPRENANT, A. & NORTH, R.A. (1998). Trinitrophenyl-substituted nucleotides are potent antagonists selective for $P2X_1$, $P2X_3$, and heteromeric $P2X_{2/3}$ receptors. *Mol. Pharmacol.,* **53,** 969–973.

VULCHANOVA, L., RIEDL, M.S., SHUSTER, S.J., BUELL, G., SURPRENANT, A., NORTH, R.A. & ELDE, R. (1997). Immunohistochemical study of the $P2X_2$ and $P2X_3$ receptor subunits in rat and monkey sensory neurons and their central terminals. *Neuropharmacology,* **36,** 1229–1242.

WERNER, P., SEWARD, E.P. & BUELL G.N. & NORTH, R.A. (1996). Domains of P2X receptors involved in desensitization. *Proc. Natl. Acad. Sci. U.S.A.,* **93,** 15485–15490.


*(Received April 18, 2002*
*Revised June 2, 2003*
*Accepted June 10, 2003)*